Archimer
http://archimer.ifremer.fr

Effect of yolk utilization on the specific gravity of chokka squid (*Loligo reynaudii*) paralarvae: implications for dispersal on the Agulhas Bank, South Africa

Rodrigo S. Martins[1, 2, *], Michael J. Roberts[1], Nicolette Chang[3], Philippe Verley[4,5], Coleen L. Moloney[2] and Erica A. G. Vida[l6]

[1] Marine and Coastal Management (MCM), Private Bag X2, Rogge Bay 8012, South Africa
[2] Zoology Department and Marine Research Institute, University of Cape Town, Private Bag X3, Rondebosch 7701, South Africa
[3] Oceanography Department, University of Cape Town, Private Bag, Rondebosch 7701, Cape Town, South Africa
[4] IRD, UR ECO-UP, Centre de Bretagne, BP 70, 29280 Plouzané, France
[5] LPO, UMR 6523 CNRS IFREMER UBO, 6 avenue Le Gorgeu, C.S. 93837, 29238 Brest Cedex 3, France
[6] Centro de Estudos do Mar (CEM), Universidade Federal do Paraná (UFPR), Caixa Postal 50.002, Pontal do Paraná PR 83.255-000, Brazil

*: Corresponding author : R. S. Martins: tel: +27 21 4307039; fax: +27 21 4342144; email address : rodrigo.plei@gmail.com

Abstract:

Specific gravity is an important parameter in the dispersal of marine zooplankton, because the velocity of currents, and therefore the speed of transport, is usually greatest near the surface. For the South African chokka squid (*Loligo reynaudii*), recruitment is thought to be influenced by the successful transport of paralarvae from the spawning grounds to a food-rich feature known as the cold ridge some 100–200 km away. The role of paralarval specific gravity on such transport is investigated. Specific gravity ranged from 1.0373 to 1.0734 g cm^{-3} during the yolk-utilization phase, implying that paralarvae are always negatively buoyant, regardless of yolk content. The data were incorporated into a coupled individual-based model (IBM)—Regional Ocean Modelling System model. The output showed that dispersal was dominantly westward towards the cold ridge. Also, modelled paralarval vertical distribution suggested that hydrodynamic turbulence was an important factor in dispersal. The negative buoyancy of early chokka squid paralarvae may reduce the risk of paralarvae being advected off the eastern Agulhas Bank and into the open ocean, where food is less abundant, so specific gravity may be important in enhancing the survival and recruitment of chokka squid.

Keywords: Agulhas Bank, chokka squid, dispersal, paralarvae, specific gravity

Introduction

According to the current understanding of the early life cycle of chokka squid (Loligo reynaudii), the survival of paralarvae hatched on the spawning grounds on the eastern Agulhas Bank is better if they are transported by currents some 100–200 km west to the "cold ridge" on the central Agulhas Bank, where primary and secondary productivity are generally high. This westward transport hypothesis linking the cold ridge to good recruitment has been supported quantitatively by Roberts (2005). However, paralarvae hatched on the deeper mid-shelf spawning grounds (Augustyn et al., 1994; Oosthuizen and Roberts, 2009) appear to face greater risk of advective loss to the adjacent oligotrophic oceanic waters than those hatched inshore, particularly within sheltered embayments (Hutchings et al., 2002; Roberts et al., 2002; Roberts and Mullon, 2010). Even given some means of return to the Agulhas Bank ecosystem for the lost paralarvae, the rates of mortality are expected to be high because squid paralarvae are particularly sensitive to food shortage (Vidal et al., 2006). Much of this thinking and experimentation has been based on the notion that squid paralarvae occupy the surface layer, where currents are faster than at depth.

Should the paralarvae be negatively buoyant, however, dispersal is likely to be more restricted and less likely to result in losses of paralarvae from the Agulhas Bank ecosystem. This has been demonstrated for marine fish and invertebrate larvae (Sclafani et al., 1997; Kelman and Emlet, 1999). Ultimately, the specific gravity of any planktonic organism will influence its vertical distribution, not only assisting in maintenance of position but also affecting differential transport patterns resulting from vertically stratified currents (Bradbury and Snelgrove, 2001; Campbell and Dower, 2003). Specific gravity, either negative or positive, can also allow some protection against visual predators whenever neutral buoyancy is achieved (Chia et al., 1984). This can affect energy usage (Chia et al., 1984; Campbell and Dower, 2003), by reinforcing or counteractive vertical swimming (Young, 1995). Also, this would be of adaptive value during the planktonic phase, because hydromechanical costs of movement can be relatively high in the viscous fluid environment in which paralarvae

are entrained, increasing the energetic cost of locomotion (Thompson and Kier, 2001). Moreover, even small changes in specific gravity are important in influencing the distribution and transport of fish eggs and larvae (Sundby, 1991; Sclafani et al., 1997; Parada et al., 2003), so the same would be expected for squid paralarvae.

As in other cephalopods, loliginid embryos develop from yolk-rich, telolecithal eggs (Boletzky, 2003), and the paralarvae hatch with a relatively large quantity of internal yolk reserves, perhaps up to 50% of their body dry weight (Vidal et al., 2002). The utilization of yolk is temperature-dependent, and there is little, if any, conversion of yolky matter into somatic tissue (Vidal et al., 2002, 2005; Martins et al., 2010). Therefore, the specific gravity of paralarvae would be affected by variation in the yolk content, influencing dispersal during the phase of yolk utilization.

The aims of this study were therefore (i) to estimate the specific gravity of newly hatched chokka squid paralarvae and changes attributable to yolk utilization and (ii) to investigate the effect of specific gravity on the horizontal dispersal of the paralarvae, with emphasis on the potential to reach the cold ridge nursery ground.

Material and methods
Egg collection, incubation, rearing procedures, and experimental design

On 18 November 2007, scuba divers collected chokka squid eggs on a spawning ground 25 m deep in St Francis Bay, South Africa. These were air-freighted to the Marine and Coastal Management (MCM) Research Aquarium in Cape Town. Travel time was 11 h, and mean water temperature was $18.88 \pm 3.90°C$. On arrival, the embryos were found to be at stage 25 of embryonic development (Arnold, 1965). The eggs were incubated for 12 d in a flow-through hatching tank, with incubation and rearing procedures and the rearing system the same as described by Martins et al. (2010). Water turnover during incubation was $42 \times$ tank volume d^{-1}, with an average temperature of $13.66 \pm 0.55°C$. A low luminosity of $13-54$ lux was maintained at the water surface. Dissolved oxygen was maintained above $7 \, mg \, l^{-1}$, and mean salinity and pH were 34.6 psu and 7.85, respectively. Nitrogenous waste levels were $5 \times 10^{-5} \, mg \, l^{-1}$ for nitrite and $0 \, mg \, l^{-1}$ for ammonia.

Most eggs hatched on 1 December 2007, defined here as experimental day 0. Paralarvae hatched earlier than that were discarded to ensure homogeneity of age. In all, 1500 paralarvae were transferred individually from the hatching tank to each of three flow-through experimental replicated tanks (referred to as the "tank line"), i.e. a total of 4500 paralarvae. The rearing temperature ($\pm$ s.d.) was $14.44 \pm 0.10°C$ for the 7-d experiment, with a maximum temperature difference of $0.1°C$ between tanks. No food was provided. A water inflow of $1.25 \, l \, min^{-1}$ was used in all experimental tanks. Water turnover during the experiment was $13 \times$ tank line volume d^{-1}. Luminosity at the water surface ranged between 37 and 98 lux. The average values of dissolved oxygen ($mg \, l^{-1}$), salinity (psu), and pH were ($\pm$ s.d.) 7.29 ± 0.26, 34.6 ± 0.17, and 7.92 ± 0.09, respectively. The nitrite level was $5 \times 10^{-5} \, mg \, l^{-1}$, with ammonia being undetectable in the rearing water during the experiment.

Measurement of settling rates and seawater specific gravity

Settling rate experiments, i.e. to determine the terminal velocity of sinking, were conducted in a temperature-controlled room at $14°C$ (the same temperature as incubation and rearing), using 75 paralarvae collected daily from the rearing tanks (25 from each tank), anaesthetized with magnesium chloride (Oestmann et al., 1997). From these, 30 were used for the settling trials and estimation of yolk content. All paralarvae from each group were subsequently used for estimating wet and dry weights (see below).

The measurements of settling rate were made in a glass column 50 cm high and 7.5 cm diameter filled with seawater collected from the rearing system and stored in a 60-l plastic bin. The water was allowed to equilibrate to room ambient temperature 3 d before the experiments. Anaesthetized paralarvae were individually collected with a pipette, visually evaluated under a microscope at $\times 20$ magnification for life signals, i.e. systemic or branchial heartbeat, then checked for tiny air bubbles or dirt attached to the body surface or trapped inside the mantle cavity. Each paralarva was then carefully placed in the column and allowed to settle for ~ 10 cm to reach terminal velocity (Zeldis et al., 1995). Settling time was recorded with a stopwatch from 40 cm down. Velocity was calculated from the slope of the plot of settling distance vs. time. Paralarvae were siphoned from the bottom of the column and placed in a plastic tray with divisions, for further measurement. The specific gravity of the water was measured with a Sea Bird SBE 19 SEACAT Profiler CTD placed into the water storage bin for 10 min before each experiment.

Body measurements, yolk weights, moisture content, survival, yolk utilization, and growth rates

Dorsal and ventral digital images of the paralarvae used in the settling experiments were recorded with a compound microscope at $\times 20$ magnification fitted with a high-resolution video system. Measurements (mm) of mantle length (ML), total length (TL), and other relevant dimensions of the paralarvae were taken using AuxioVision LE© (4.1 version) image analysis software. Measurements of the anterior and the posterior internal yolk sac were taken from the ventral images. The volume of the yolk sac was estimated by superimposing the standard geometric forms on the body shapes (Vidal et al., 2002, 2005), and yolk wet weight was calculated by multiplying the yolk volume by a specific gravity of $1.036 \, g \, cm^{-3}$ (O'Dor et al., 1986).

Wet and dry weights of the paralarvae were obtained using a Sartorius A120S analytical balance, as described by Martins et al. (2010). Every day, 15 groups of 5 paralarvae each were weighed; wet weight was estimated by dividing the total weight by the number of squid in each group. Similarly, dry weights were obtained after drying the paralarvae in an oven at $60°C$ for 20 h and cooling in a desiccator for 4 h. Moisture content was expressed as the difference (%) between the wet and the dry weights.

Mortality was determined daily by siphoning dead paralarvae from the bottom of the tanks, and survival was estimated as the percentage of live paralarvae left in each tank relative to the initial number of paralarvae (1500), excluding those sampled for data collection. Yolk utilization and growth rates (daily instantaneous, in % d^{-1}) were determined by fitting a standard exponential model to data on wet-weight-at-age and yolk-at-age (Vidal et al., 2002).

Estimating the specific gravity of paralarvae

There were limits to estimating the three-dimensional shape of a squid paralarva accurately, so several assumptions had to be made:

(i) paralarvae were assumed to approximate a rotational ellipsoid in form (Figure 1), and volume (V) was estimated using the formula $V = 0.1667\,\pi LH^2$ (Heming and Buddington, 1988);

(ii) the major axis (L) was assumed to be the length between the mantle tip and the base of the fourth pair of arms, and the height (H) was measured halfway along the major axis (measurements were made with the animal in the ventral position and the mantle relaxed; Figure 1);

(iii) as the bulk of paralarval weight is contained in the head and mantle, the fins and arms were not considered in the calculations;

(iv) the diameter (d) of the spherical particle used in subsequent equations was based on the radius of a sphere with the same volume as the ellipsoid (Tanaka, 1992);

(v) the resistance for spheres ranges between 95 and 110% of ellipsoids (McNown and Malaika, 1950), so it was assumed that the resistance of a sphere is equal to that of an ellipsoid in a viscous fluid (Tanaka, 1992).

To determine the applicability of the Stokes equation for estimating the specific gravity of paralarvae, the Reynolds number (Re), a non-dimensional index that characterizes the relative importance of inertial forces and viscous forces on a body embedded in a fluid environment (Mann and Lazier, 1991), was calculated for each transformed spheroid particle using the formula (Moore and Villareal, 1996)

$$\mathrm{Re} = \frac{wd}{v/\rho_w}, \tag{1}$$

where d (cm) is the diameter of the transformed spheroid particle, w (cm s^{-1}) the settling velocity (corrected, see below), v the seawater molecular viscosity (0.01 g s^{-1} cm^{-1}; Tanaka, 1992), and ρ_w the specific gravity of seawater (g cm^{-3}). The result was that all transformed spheroid particles had a Re $>$ 0.5 (range: 1.93–3.91; average: 2.66 $\pm$ 0.39 s.d.), which meant that the traditional Stokes equation could not be used (Sundby, 1983) and that an adapted equation had to be used.
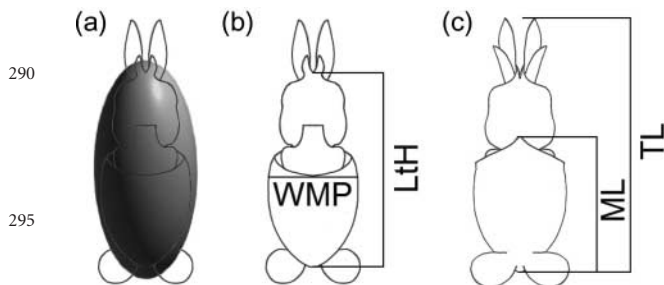
Figure 1. The approximate ellipsoid form concept and measurements for *L. reynaudii*. (a) Schematic drawing of the approximate ellipsoid concept. (b) Measurements taken on ventral side for the ellipsoid volume calculation. (c) Measurements taken on the dorsal side. LtH, length between the tip of the mantle and the base of the fourth arm pair (=ellipsoid major axis L); WMP, width of the middle point (=ellipsoid height H); ML, dorsal mantle length; TL, total length.

The observed settling velocities (in cm s^{-1}) in the glass column were biased because of wall and end effects, so they were corrected using the formula proposed by Cambalik *et al.* (1998):

$$w_\infty = w\left(1 + 2.4\frac{r}{R}\right)\left(1 + 3.3\frac{r}{h}\right), \tag{2}$$

where w is the settling velocity, w_∞ the settling velocity in a medium of infinite width and height, r and R the radii of the transformed spheroid particle and the apparatus, respectively, and h the height of the measured volume.

The specific gravity of the paralarvae (ρ_p) was then estimated from the transformed spheroid particles and settling velocity data, using the formula (Sundby, 1983):

$$w = K_I d_0 (\rho_p - \rho_w)^{2/3} v^{-1/3}, \tag{3}$$

where K_I is a constant approximately equal to 19, $d_0 = d - D\zeta$, where d is the true diameter of the paralarva, D the uppermost limit of size where the Stokes equation applies (i.e. 0.6 mm), and ζ a constant equal to 0.4 for spheres.

The effect of specific gravity on dispersal of paralarvae

A Regional Ocean Model System (ROMS) coupled to an individual-based model (IBM) was used to investigate the effect of specific gravity on the dispersal of squid paralarvae.

Hydrodynamic model

An ROMS has previously been configured for the region 2.5°W to 54.8°E and 4.8–46.8°S by Penven *et al.* (2006) and is referred to as the Southern African Experiment (SAfE). ROMS is a self-explicit, free-surface, hydrostatic, primitive equation ocean model (Shchepetkin and McWilliams, 2005), and it uses stretched terrain-following coordinates in the vertical domain and orthogonal curvilinear coordinates in the horizontal direction (Song and Haidvogel, 1994). Horizontal resolution is 1/4°, and it ranges from 19 km in the south to 27.6 km in the north. Vertical resolution is high at the surface (0.37–5.70 m) and coarse (11–981 m) in the bottom layers, with 32 s-coordinate levels between the surface and the bottom.

GEBCO (General Bathymetric Chart of the Oceans) data were used for bottom topography. The model started from rest and was forced at the surface using the comprehensive ocean-atmosphere dataset (COADS) monthly climatology (Da Silva *et al.*, 1994) and the WOA (World Ocean Atlas) temperature and salinity data (Conkright *et al.*, 2002). As the model took 2 years to reach statistical equilibrium, only output data from years 3 to 10 were used. More details on the structure and functioning of SAfE are given in Lett *et al.* (2007) and Chang (2008).

As this study required high resolution to reproduce coastal hydrodynamics on the eastern Agulhas Bank, particularly in the embayments and near the cold ridge, a child model was extracted from the parent model for the area between 11.6 and 27.4°E and 27.7 and 38.8°E (Figure 2). The child model had a temporal and spatial resolution three times higher than the parent model, with 160×190 gridpoints in the horizontal direction, and 32 vertical levels. This yielded a horizontal resolution of 1/12° (~8 km). The boundary conditions of the child grid were supplied by the parent grid. A full description of the child configuration is given in Chang (2008).
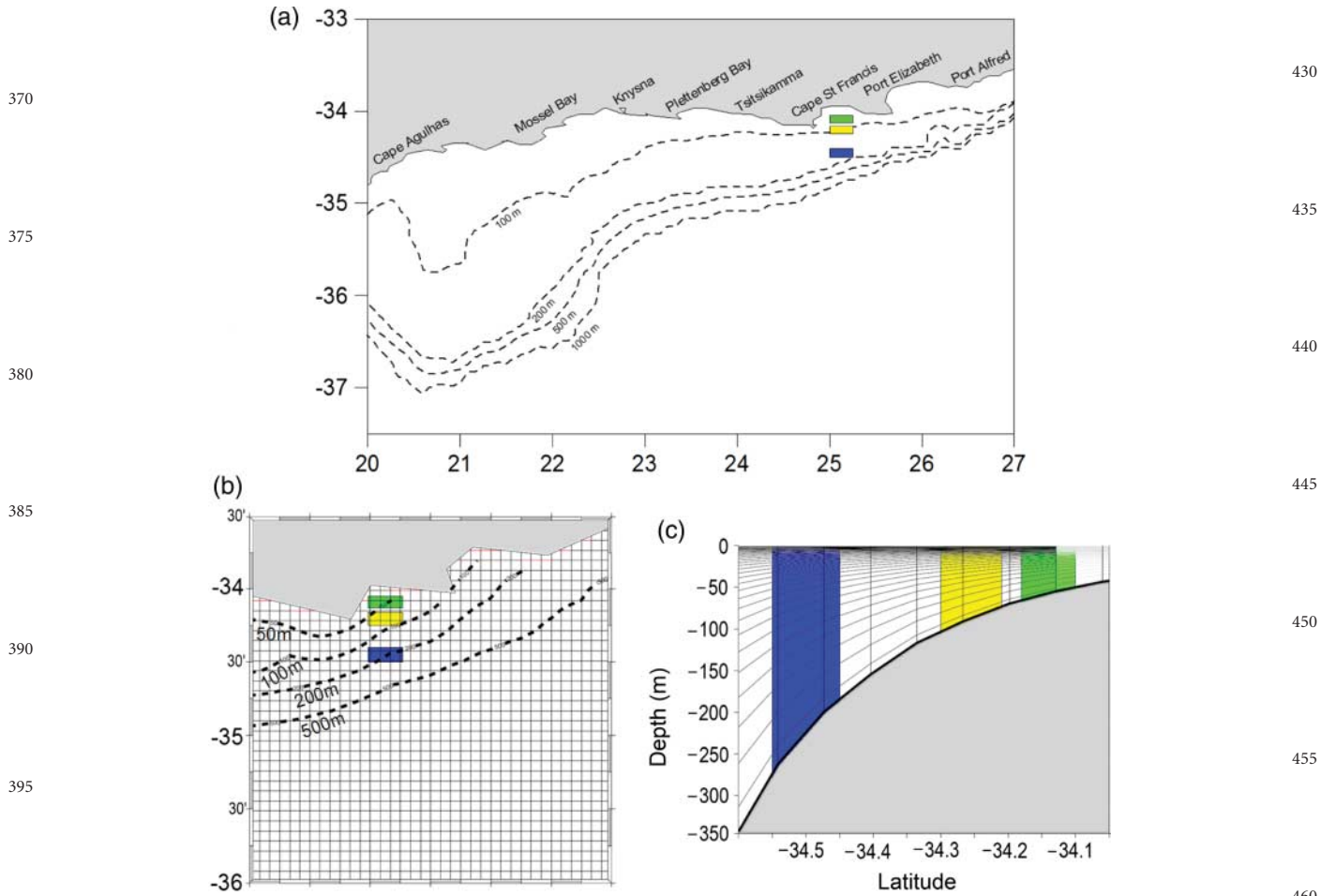
Figure 2. Particle release areas. (a) Geographic position of Bay In (green), Bay Off (yellow), and Mid-Shelf (blue). (b) Horizontal (close-up, coloured rectangles), and (c) vertical grids (meridional section across 25.1667°) of the regional domain of the SAfE ROMS model, showing the release areas (coloured columns).

The SAfE configuration of ROMS has been validated by Penven et al. (2006), and it was shown that all known large and mesoscale oceanographic features in the region reproduced and compared well with field and satellite data. For instance, the simulated transport volume in the Agulhas Current compared well with that determined by field measurements (Bryden et al., 2005); the Agulhas Return Current is at the correct latitude (Lutjeharms and Ansorge, 2001) and exhibits meanders at observed longitudes (Boebel et al., 2003); and the model mean sea surface height (SSH) matches the observed SSH derived from hydrographic data, surface drifter velocities, altimetry, and a geoid model (Rio and Hernandez, 2004).

Individual-based model

The effect of the specific gravity on dispersal of paralarvae was assessed using the open source Ichthyop software (2.1.1 version). This tool tracks passive movements of Lagrangian particles using velocity fields stored from hydrodynamic model simulations i.e. ROMS (Lett et al., 2008). The outputs generated by Ichthyop record the position (latitude and longitude), depth, temperature, and salinity experienced by each tracked particle embedded within the hydrodynamic fields of the model. The performance of Ichthyop has been tested (i) by tracking particle trajectories in

an artificially uniform velocity field and (ii) by comparing with another offline Lagrangian tool (see details in Lett et al., 2007). The program was modified to change particle specific gravity with age, according to the formula

$$\text{Sp.gr.} = 1.0539 \, e^{-0.0018a}, \tag{4}$$

where Sp. gr. is the specific gravity (in g cm^{-3}) and a the age in days after hatching. This meant that the specific gravity of particles ranged from 1.054 to 1.043 g cm^{-3} during the 7-d simulations in this study.

Particles were released at three locations off St Francis Bay, defined in Figure 2 by rectangles of ~8 km × 19 km (~152 km^2), and termed Bay In, Bay Off, and Mid-Shelf. Bay In and Bay Off were spaced 2.5 km apart, and Mid-Shelf was 17 km from Bay Off. These areas were chosen not only to straddle the depth range of the spawning grounds between 20 and 120 m, but also to be inclusive of an embayment (Oosthuizen and Roberts, 2009). Moreover, the areas are known spawning sites for chokka squid (Roberts and Sauer, 1994; Roberts et al., 2002). The depth at these sites ranged between 35 and 80, 86 and 124, and 110 and 130 m, respectively. The release areas encompassed 4–8 gridpoints of the child SAfE model (Figure 2).

In all, 15 000 particles were released during each simulation, i.e. 5000 particles per release area. No diffusion terms, biological, or behavioural characteristics were included in the simulations, resulting in passive particle movement only (i.e. Lagrangian). As chokka squid eggs are benthic, particles in the model were released in the bottom layer, i.e. 34 m at Bay In, 85 m at Bay Off, and 109 m at Mid-Shelf. Simulations were run using child model years 3, 7, and 10, and only the month of November, when spawning activity normally peaks (Augustyn *et al.*, 1994).

Particles were released once per week for 4 weeks and tracked for 7 d. To assess the importance of buoyancy for dispersal, simulations were performed with particles that changed specific gravity and with particles that were neutrally buoyant. Dispersal was characterized horizontally and expressed as the average displacement distance from the release areas. Displacement distances between initial and final positions of each non-beached particle were calculated from Koordinaten.de (2008):

$$\text{Displacement distance} = \delta \times 6378.137 \text{ km}, \quad (5)$$

where 6378.137 km is the radius of the equator and δ the distance (in radians) between two geographical locations, assuming a spherical shape of the planet, calculated as follows:

$$\delta = \text{ArcCos}[\text{Sin}(-\text{Lat}_1) \times \text{Sin}(-\text{Lat}_2) + \text{Cos}(-\text{Lat}_1) \\ \times \text{Cos}(-\text{Lat}_2) \times \text{Cos}(\text{Long}_2 - \text{Long}_1)], \quad (6)$$

where $\text{Lat}_1 - \text{Long}_1$ and $\text{Lat}_2 - \text{Long}_2$ are the radian-transformed coordinates of initial and final positions of each particle.

The numbers of particles retained within each release area and beached were also recorded. The effect on dispersal distance of the release area, week, year, and specific gravity and factor interactions were assessed with a multifactor ANOVA, allowing several levels of interactions, to gain insights from the global model (Lebreton *et al.*, 1992).

Modelled vertical distribution

Composite vertical profiles for each release area, showing the concentration of particles in 10 m layers, were calculated from model outputs for all 7-d simulations, i.e. for all 3 years. As the data did not match the conditions of normality and homoscedasticity, differences in particle depth concentrations between varying specific gravity and neutrally buoyant particles were compared with a non-parametric Mann–Whitney *U*-test (Zar, 1996).

Results

Mean ($\pm$ s.d.) body measurements of paralarvae at hatching were 2.54 $\pm$ 0.08 mm ML and 4.97 $\pm$ 0.11 mm TL. Wet, dry, and yolk weights were 2.02 $\pm$ 0.09, 0.40 $\pm$ 0.04, and 0.26 $\pm$ 0.10 mg, respectively. Yolk was exponentially utilized at an instantaneous rate of 32% d^{-1} and was exhausted 6–7 d after hatching (Figure 3). Body weight followed the same trend, with a weight loss rate of 10% d^{-1} (data not shown). Mortality peaked on Day 5 at 80%. Daily changes in specific gravity were best modelled by an exponential function (Figure 3), and the moisture levels of paralarvae increased while specific gravity decreased with age (Figure 4).

The relationships between specific gravity, yolk, and body weight are depicted in Figure 5. Log-linear functions provided the best fit to these data. It is clear that the yolk content
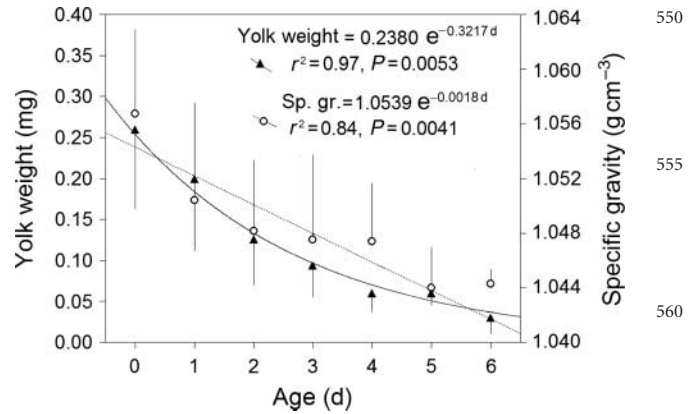
Figure 3. Yolk utilization of *L. reynaudii* (open circles, continuous line) and changes in specific gravity (filled triangles, dotted line) at 14.44 $\pm$ 0.10°C (s.d.). Values are the means of 29–30 paralarvae $\pm$ s.d. Age is expressed as days post-hatch.
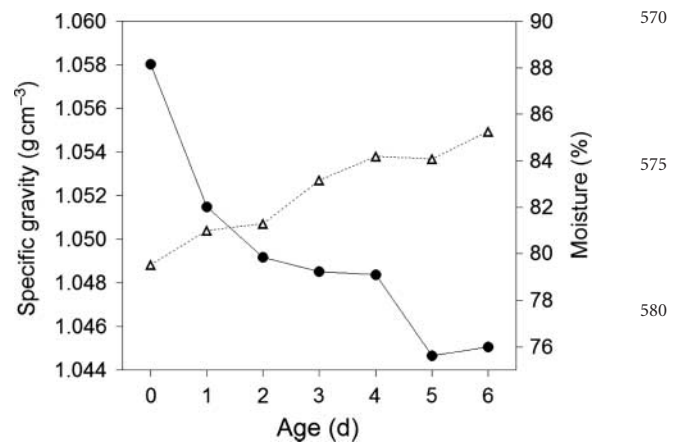
Figure 4. Specific gravity (dots) and percentage moisture content (open triangles) plotted against age of *L. reynaudii*. Specific gravity values are the means of 29–30 paralarvae, and moisture values the means of 15 groups of five paralarvae each. Age is expressed as days post-hatch.

($p < 0.05$) explained much of the variability in the specific gravity measurements, evidenced by large coefficients of determination ($r^2 > 0.60$) for the fitted curves (Figure 5a and b). This fit **Q2** deteriorated ($r^2 = 0.48$; Figure 5c) when yolk content was removed from the body weight, which suggested that the yolk content accounts for some of the variability in specific gravity.

The effect of varying specific gravity relative to neutral buoyancy on particle dispersion is shown in the composite model simulation plots of Figure 6. Irrespective of buoyancy, the data show that most of the dispersal was westwards for all three release areas. Interestingly, some particles with a varying specific gravity released on the mid-shelf were transported eastwards to Algoa Bay (Figure 6c). In general, the neutrally buoyant particles dispersed over greater areas relative to their negatively buoyant counterparts. Notably, particles released at the Mid-Shelf site were transported farthest, resulting in dispersal over much of the eastern and outer central Agulhas Bank (Figure 6c). Some particles even left the shelf (i.e. past the 200-m isobath) at the southern tip of the Agulhas Bank.
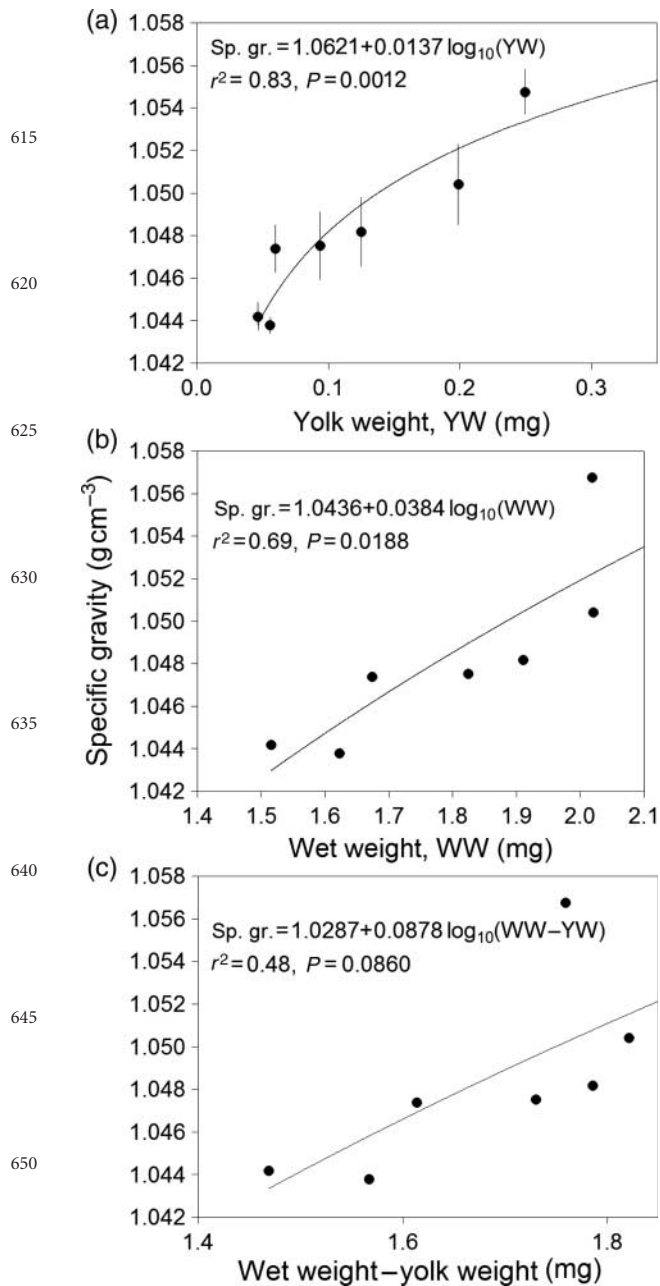
Figure 5. Specific gravity plotted against (a) yolk weight, (b) wet weight, and (c) wet weight minus yolk weight of *L. reynaudii*. Values of specific gravity and yolk weight are the means of 29–30 paralarvae. Wet weight values are the means of 15 groups of five paralarvae each. The vertical bars in (a) represent the s.d.

Dispersal distance increased between the inshore and the off-shore release sites (Table 1). Distance covered by the particles with varying specific gravity, on average, was shorter than their neutrally buoyant counterparts. This was especially evident for the Mid-Shelf release area, where the overall distance travelled by particles with varying specific gravity were 1.7 times shorter than, and the associated variance nearly half that of, the neutrally buoyant particles (Table 1). Also, the relative retention of particles in the release rectangles and those beached decreased from inshore to offshore. Interestingly, the proportion of particles retained and

beached was higher for particles with varying specific gravity than for those that were neutrally buoyant (Table 1). Of the variables in the analysis, release area (18.75%), followed by specific gravity (1.85%), and all the situations where those two variables interacted, accounted for the greatest variance in the model (Table 2). All the other variables and their interactions, although statistically significant, were each responsible for <1% of the variance (Table 2).

Composite vertical profiles for the concentration of particles in 10 m layers after 7 d are shown in Figure 7. Except Bay Off (neutral), most particles remained at the release depth. The largest difference in behaviour between the neutrally buoyant and varying specific gravity particles was at the Bay In site, where the former moved up into the water column. The negative buoyancy of the latter appears to have prevented particles from entering the surface layer. The difference in behaviour between particle types was less marked at the other two sites. Note that the distributions of particles below the release depth were attributable to the sloping bathymetry either side of the release point in the demarcated areas. For the Bay In, Bay Off, and Mid-Shelf areas, the depth differences between the shallowest and the deepest boundaries were 50, 38, and 20 m, respectively.

Perhaps of some importance is the tendency for negatively buoyant particles to be more concentrated in the lower water column (i.e. 60–90 m) at the Mid-Shelf site. Statistically, the vertical distribution of neutrally buoyant particles and particles of varying specific gravity differed significantly in all release areas (the Mann–Whitney U-test, $p < 0.05$).

Discussion
Specific gravity of paralarvae vs. yolk utilization
The results showed that chokka paralarvae always have a specific gravity greater than the surrounding seawater in the rearing tanks ($\Delta\rho = 0.0193-0.0310 \text{ g cm}^{-3}$). The specific gravity of paralarvae was strongly influenced by the yolk content and changed with its utilization, i.e. specific gravity decreased as the yolk was utilized. Concomitantly, the water content of paralarvae increased.

Similar relationships have been found for a number of fish species, including Atlantic salmon (*Salmo salar*; Peterson and Metcalfe, 1977), Atlantic cod (*Gadus morhua*; Ellertsen *et al.*, 1980), Atlantic herring (*Clupea harengus*; Henri *et al.*, 1985), goby (*Sicydium punctatum*; Bell and Brown, 1995), and striped trumpeter (*Latris lineate*; Trotter *et al.*, 2005). As in chokka squid paralarvae, specific gravity in all these fish larvae is greatest at hatching, then decreases to a minimum at yolk exhaustion. A difference between chokka squid and fish, however, is that the changes in the specific gravity of fish larvae driven by yolk utilization seem to be related to the utilization of yolk for somatic growth (Heming and Buddington, 1988). In contrast, squid paralarvae do not appear to convert yolky matter into somatic tissue (Vidal *et al.*, 2002), implying that the observed decrease in specific gravity and concomitant increase in water content are caused by catabolism of internal yolk of high specific gravity (and low in moisture) to fuel metabolism.

A comparison between the specific gravity of chokka squid paralarvae and several fish and invertebrate larvae and holoplanktonic crustaceans is given in Table 3. This evaluation shows that chokka paralarvae are heavier than most of the organisms listed, but lighter than the ostracod *Conchoecia* sp. and heavy-shelled invertebrate larvae. Chokka squid paralarvae have a similar
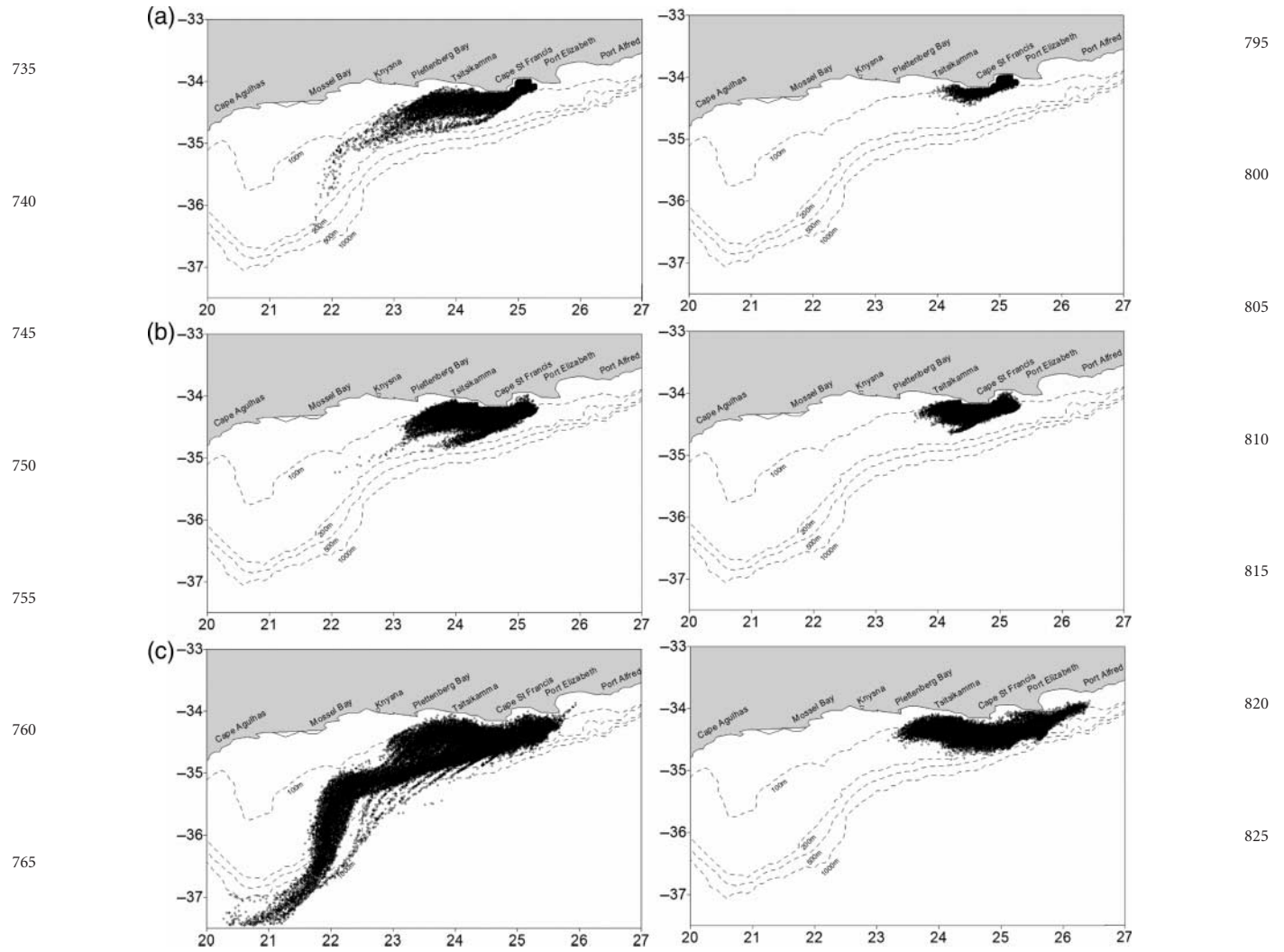
Figure 6. Composites of particle dispersal for all 7-d simulations conducted during November in model years 3, 7, and 10 for the three release sites: (a) Bay In, (b) Bay Off, and (c) Mid-Shelf. Dots represent the final particle positions after 7 d. Left panels, neutrally buoyant particles; right panels, particles of varying specific gravity ($1.054 - 1.043$ g cm^{-3}).

Table 1. Mean dispersal distance (and variance in km^2) for the Lagrangian experiment by site and year, giving also the overall proportions of particles retained in the release areas and beached.

	Dispersal distances (km)					
Release area	Year 3	Year 7	Year 10	Dispersal distances across all years	% retained	% beached
Neutrally buoyant particles						
Bay In	17.1 (461.48)	17.5 (372.4)	17.7 (444.3)	17.4 (422.8)	5.2	16.8
Bay Off	15.5 (243.9)	14.4 (202.4)	15.6 (236.7)	15.1 (228.1)	5.1	0.7
Mid-Shelf	51.8 (2 188.3)	42.0 (1 406.9)	68.6 (3 675.2)	53.9 (2 526.9)	4.4	0.02
Varying specific gravity particles						
Bay In	11.8 (89.1)	11.8 (81.4)	12.2 (97.2)	11.9 (89.0)	6.0	18.5
Bay Off	11.1 (93.1)	10.3 (76.8)	11.3 (97.0)	10.9 (89.3)	5.8	1.2
Mid-Shelf	37.7 (1 828.1)	36.7 (1 244.6)	21.4 (392.5)	31.9 (1 209.9)	5.4	0.04

range of specific gravity to that of demersal Atlantic salmon (*S. salar*) larvae. However, their mean specific gravity (1.0483 g cm^{-3}) is close to the mean specific gravity (1.0463 g cm^{-3}) of Pacific bluefin tuna (*Thunnus orientalis*) larvae of similar size ($\sim$5 mm TL), which are planktonic (Takashi *et al.*, 2006). Additionally, concentrations of *Doryteuthis opalescens* paralarvae off California have been found in depths between 15 and 30 m, which suggest a midwater, planktonic habitat (Zeidberg and Hamner, 2002). This observation implies that specific gravity *per se* may not determine the vertical

Table 2. Multifactor ANOVA results for the Lagrangian experiment showing the contributions of the different variables to determining modelled passive dispersal.

Variables and terms	Sum of squares	d.f.	Mean square	F-value	p-value	% variance explained
Intercept	112 631 253	1	112 631 253	136 427.5	<0.01*	
Single variable						
Specific gravity	5 770 409	1	5 770 409	6 989.6	<0.01*	1.85
Release area	58 525 540	2	29 262 770	35 445.3	<0.01*	18.75
Year	229 632	2	114 816	139.1	<0.01*	0.07
Week	466 882	3	155 627	188.5	<0.01*	0.15
Interaction terms						
Specific gravity × Release area	5 240 520	2	2 620 260	3 173.9	<0.01*	1.68
Specific gravity × Year	1 871 507	2	935 753	1 133.5	<0.01*	0.60
Specific gravity × Week	841 159	3	280 386	339.6	<0.01*	0.27
Release area × Year	353 010	4	88 253	106.9	<0.01*	0.11
Release area × Week	1 141 113	6	190 185	230.4	<0.01*	0.37
Year × Week	450 573	6	75 096	91.0	<0.01*	0.14
Specific gravity × Release area × Year	5 453 815	4	1 363 454	1 651.5	<0.01*	1.75
Specific gravity × Release area × Week	1 265 772	6	210 962	255.5	<0.01*	0.41
Specific gravity × Year × Week	2 428 710	6	404 785	490.3	<0.01*	0.78
Release area × Year × Week	1 440 686	12	120 057	145.4	<0.01*	0.46
Specific gravity × Release area × Year × Week	3 665 217	12	305 435	370.0	<0.01*	1.17
Error	223 055 709	270 182	826			71.45
Total	312 200 254					

% variance explained: $100 \times SS_{Effect}/SS_{Total}$.
*Significant at $p < 0.01$.
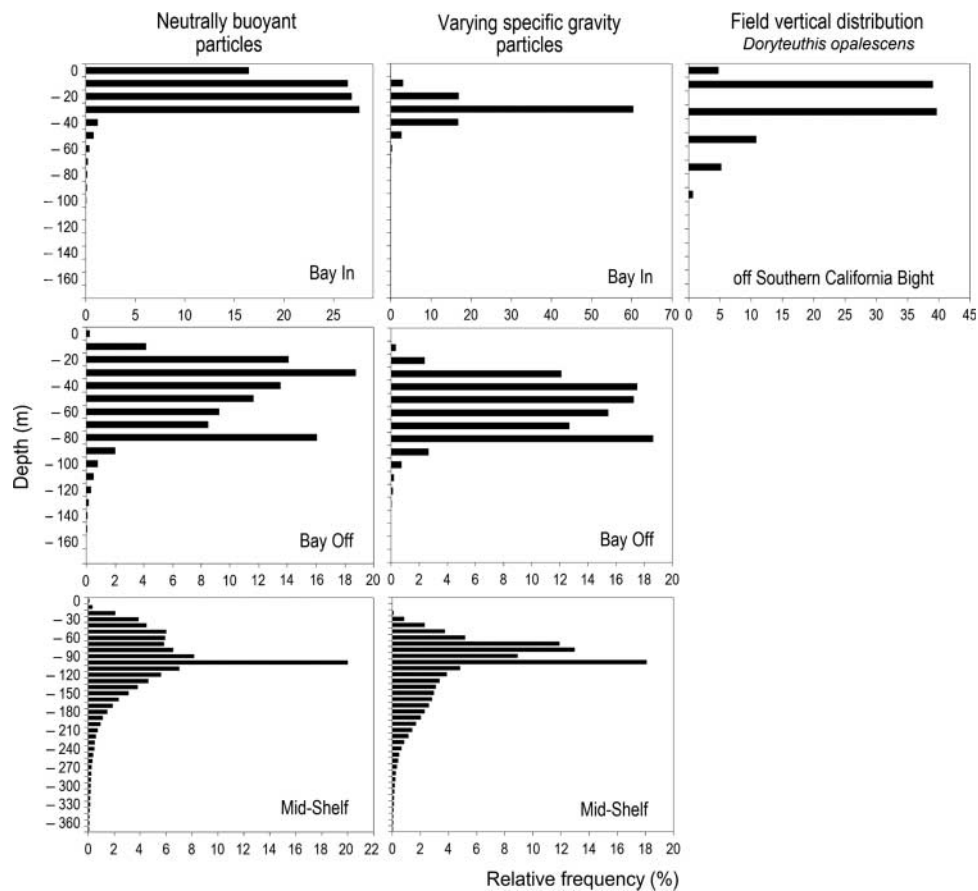
Figure 7. Composite vertical distributions of neutrally buoyant and varying specific gravity particles in the model (in 10 m layers) after 7 d for the three release areas, i.e. the data for all years are combined. Note that x-axis scales vary. Particles were released near the bottom at depths of 34, 84, and 109 m, respectively. Field data for *D. opalescens* paralarvae are included for comparative purposes and were drawn from Zeidberg and Hamner (2002).

Table 3. Comparison of the estimated specific gravity of *L. reynaudii* paralarvae and some fish and invertebrate larvae, an ostracod and some calanoid copepods.

Taxon	TL (mm)	Specific gravity (g cm^{-3})	Specific gravity of seawater (g cm^{-3})	Mean temperature (°C)	Habitat
Osteichthyes					
Atlantic cod (*Gadus morhua*)[a]	5.75	1.0275*	1.0265	5	Planktonic
Atlantic salmon (*Salmo salar*)[b]	15.00 – 30.00	1.0460 – 1.0675	–	15	Demersal
Blue whiting (*Micromesistius poutassou*)[c]	<2.00	1.0282**	–	10	Planktonic
Halibut (*Hippoglossus hippoglossus*)[d]	6.00 – 7.00[e]	1.0206**	1.0240	5	Neustonic
Japanese eel leptocephali (*Anguilla japonica*)[f]	3.40 – 56.60	1.0190 – 1.0250	1.0240	22	Neustonic
Leptocephali larvae (six species)[f]	21.70 – 185.10	1.0280 – 1.0430	1.0240	22	Neustonic
Pacific blue tuna (*Thunnus orientalis*)[g]	3.00 – 3.80	1.0278	–	–	Planktonic
Pacific blue tuna (*Thunnus orientalis*)[g]	5.60	1.0463***			
Striped trumpeter (*Latris lineata*)[h]	<5.30	1.0265 – 1.0290****	1.0265	16.4	Neustonic
Echinodermata					
Cushion star (*Pteraster tesselatus*)[i]	–	1.0220 – 1.0240	1.0220	12.2	Planktonic
Sand dollar (*Dendraster excentricus*)[j]	–	1.2500	–	–	Planktonic
Polychaeta					
Terebellid polychaete (*Eupolymnia nebulosa*)[k]	–	1.0080 – 1.0120	–	16	Planktonic
Tomopterid polychaete[f]	3.80	1.0470	1.0240	22	Planktonic
Mollusca					
Chokka squid (*Loligo reynaudii*)	4.45 – 5.29	1.0373 – 1.0734	1.0258	14.3	?
Giant scallop (*Placopecten magellanicus*)[l]	–	1.2600 – 1.3400*****	–	–	Planktonic
Gould shipworm (*Bankia gould*)[m]	–	1.1920*****	–	20	Planktonic
Unidentified oceanic squid paralarvae[f]	7.00******	1.0610	1.0240	22	Planktonic
Crustacea					
Halociprid ostracod *Conchoecia* sp.[f]	2.20	1.2400	1.0240	22	Planktonic
Unidentified calanoid copepods[f]	2.00 – 4.90	1.0580 – 1.0610	1.0240	22	Planktonic

Values of TL and specific gravity are averages and, where data are available, ranges. –, no data.
[a]Sclafani *et al.* (1993).
[b]Peterson and Metcalfe (1977).
[c]Ådlandsvik *et al.* (2001).
[d]Magnor-Jensen and Huse (1991).
[e]Blaxter *et al.* (1983).
[f]Tsukamoto *et al.* (2009).
[g]Takashi *et al.* (2006).
[h]Trotter *et al.* (2005).
[i]Kelman and Emlet (1999).
[j]Pennington and Emlet (1986).
[k]Nozais and Duchêne (1996).
[l]Gallager *et al.* (1996).
[m]Gallager (1985).
*At yolk sac exhaustion.
**Newly hatched larvae.
***Post yolk larvae.
****Before feeding/swimbladder inflation.
*****Pediveliger.
******From the tip of the mantle to the base of the first arm pair.

distribution of squid paralarvae in the water column and that species-specific swimming, vertical migration behaviour, and local hydrodynamics (Franks, 1992) are just as important.

Also of interest in the results of the present study is the deviation of specific gravity (as yolk is utilized) from the standard exponential decay model, with some indication of a discontinuity after 4 d (Figure 2). This could be accounted for by selective utilization of yolk components, already observed in fish and invertebrate embryos, and larvae (Kamler, 2008; Martínez *et al.*, 2008). For *L. reynaudii*, no data on the biochemical profiles of the yolk are available, but cephalopod yolk is composed mostly of phospholipoproteins (Lee, 1991). Protein is catabolized for energy production preferentially over lipids (Nelson and Cox, 2004), and this would be particularly true in cephalopods, which have a vigorous protein-based metabolism (Lee, 1994). As buoyancy is sensitive to the biochemical composition of fish larvae and invertebrate zooplankton, it is proposed that the specific gravity trend we observed was caused by the selective use of yolk components (Yin and Craik, 1992; Campbell and Dower, 2003). This trend is illustrated schematically in Figure 8.

In our study, specific gravity was shown to be a function of yolk content in newly hatched paralarvae, but there are other variables that may need to be considered to refine this work. First, independent of yolk content, specific gravity may vary with a circadian cycle reflecting the physiological condition of paralarvae (Vidal *et al.*, 2006), as observed in fish larvae (Sclafani *et al.*, 1997; Hare *et al.*, 2006). Second, fed paralarvae may show changes in specific gravity in a different manner from starved paralarvae during the yolk-utilization phase. This is due apparently to the slower utilization of yolk in fed paralarvae (Vidal *et al.*, 2002, 2005). Also, specific gravity may be temporarily influenced by the type of food in the gut of paralarvae. Finally, the specific
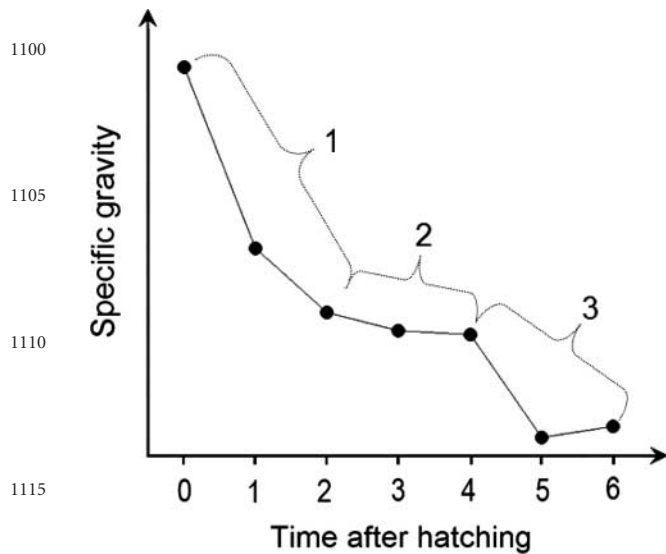
Figure 8. Conceptual hypothetical schematic phases in the changes in the body specific gravity in *L. reynaudii* paralarvae, based on the data showed in Figures 1 and 2. (1) Initial phase, high energy expenditure owing to active jetting to the surface (Vidal *et al.*, 2005), with the protein components of the yolk catabolized quickly and dramatic changes in the specific gravity. (2) Intermediate phase, lipid and protein components become evenly distributed, and there is a slowing of the variation in the specific gravity. (3) Final phase, protein components are exhausted and the yolk is mainly lipidic in composition, with dramatic changes in the specific gravity.

gravity of paralarvae could be affected by temperature-induced changes in the density of the aqueous component of paralarva tissues, as in fish eggs and larvae (Peterson and Metcalfe, 1977; Zeldis *et al.*, 1995).

Horizontal dispersal vs. specific gravity

Horizontal dispersal in the simulations was mostly westward and subsurface for both inshore and offshore release areas. This supports the westward transport hypothesis proposed by Roberts (2005), which postulates that squid paralarvae hatched on the eastern Agulhas Bank spawning grounds will be transported by currents passively towards the central Agulhas Bank where there is a nursery ground for the paralarvae near the food-rich cold ridge. It is important to remember that no biological attributes were assigned to the particles, so the results reflect only the effect of varying specific gravity. Also, simulations were designed to cover the duration of the yolk reserve only, and the fate of particles thereafter was not assessed.

The simulations clearly show that release area is an important factor influencing dispersal, with particles released on the mid-shelf spreading wider and travelling farther than those released inshore. Particle buoyancy was similarly important, with specific gravity reducing dispersal and retaining particles closer to shore. Hence, there was no leakage to offshore, oceanic waters, in contrast to the fate of the neutrally buoyant particles. It is also important to note that these results improve on those of Roberts and Mullon (2010), who ran the first Lagrangian ROMS–IBM for chokka squid. In that study, the early versions of ROMS (referred to as PLUME; Penven *et al.*, 2001) and the IBM (which has now been developed into Ichthyop) were used, and in the absence of high resolution of the model and information on specific gravity, it showed large losses of neutrally buoyant particles from the eastern Agulhas Bank to the open ocean.

Within the context of the westward transport hypothesis and the early life cycle of chokka squid, specific gravity would seem to play an important role by maintaining paralarvae inshore on the eastern Agulhas Bank, where feeding conditions are thought to be more favourable during passive transport to the nursery ground on the central Agulhas Bank. Such behaviour would offset paralarva starvation, which is very possible during the first few days post-hatch, i.e. during the "no net growth" phase (Vidal *et al.*, 2002), and improve recruitment success.

Modelled vs. observed vertical distribution

Both particle types in the model were distributed throughout the water column—as opposed to particles remaining only in the bottom layer, where they were introduced. Given that particles were neutrally or negatively buoyant and had no swimming capabilities, such a distribution can only be possible as a result of hydrodynamic turbulent mixing. Turbulent mixing has been invoked as a factor that assists in the maintenance of vertical position for negatively buoyant squid paralarvae and ichthyoplankton by a number of authors, e.g. Zuev (1964), Sundby (1991), and Zeidberg and Hamner (2002). Chokka squid paralarvae held in aquaria continuously jet in the vertical dimension to maintain height in the water column under quiescent hydrodynamic conditions, which verifies the specific gravity values obtained in this study. Jetting, however, is costly in terms of energy, and when resting, the paralarvae sink to the tank bottom. Such benthic behaviour is not observed in the model results, so it would appear that although specific gravity increases the downward force on a particle, hydrodynamic turbulence produces an (greater) upward force component such that the particles become dispersed higher into the water column. This would account for the similar vertical distribution patterns between the neutrally buoyant particles and those with a greater specific gravity, shown in Figure 7.

To check the correctness of turbulence in the ROMS, and hence the IBM vertical distribution results, field depth data for *D. opalescens* paralarvae from Zeidberg and Hamner (2002) were included in this study. *Doryteuthis opalescens* lives off the west coast of the United States. Their paralarvae were sampled in a range depth between 50 and 100 m and are shown as a composite in Figure 7. A similarity between the modelled distributions and the field data exists in so far as both are found throughout the water column, including the surface layer, which supports the notion that turbulence plays a role. However, the trend in the field data is also asymmetrical, with more *D. opalescens* paralarvae being closer to the shallower depths. This contrasts the modelled results for the varying specific gravity particles at both the Bay In and the Bay Off sites and suggests a degree of self-manoeuvrability by the live paralarvae towards the surface. It would therefore seem that both hydrodynamic turbulence and swimming account for the distribution of squid paralarvae in the water column. Future work needs to investigate the swimming ability of squid paralarvae as a function of age.

Although the role of turbulence has been stressed, it is important to note that a significant proportion of model particles, both neutrally and negatively buoyant, still remained at the release depth, and this was particularly obvious at the deeper Mid-Shelf release site (i.e. 109 m). This suggests that the extent of turbulence reproduced in the ROMS configuration is realistic because it

produces a time-dependent diffusion pattern of particles over the 7-d simulation, as opposed to a homogenous distribution, which would be unrealistic.

Conclusions

This study greatly improved on the first Lagrangian particle tracking simulations undertaken by Roberts and Mullon (2010) in which a primitive ROMS–IBM was used with neutrally buoyant particles to represent squid paralarvae. Of concern in the earlier results were the observed high advective losses of particles from the eastern Agulhas Bank to the open ocean, and the dire consequence that would have on recruitment. In the present study, however, we showed experimentally that chokka squid paralarvae are negatively buoyant when hatched and that their specific gravity decreases as yolk is utilized, but always remains greater than that of seawater. Simulations from the newer Ichthyop Lagrangian tracking IBM configured together with an improved version of ROMS specifically for the eastern Agulhas Bank (the main spawning grounds of chokka squid) showed neutrally buoyant particles for both inshore (embayment) and mid-shelf release sites dispersing west towards the central Agulhas Bank, where zooplankton (food) is more abundant. This finding supports the westward transport hypothesis of Roberts (2005), at least during peak spawning in November, for which the simulations were run.

The new simulated dispersal plume for the neutral particles released on the mid-shelf extends offshore at the southern tip of the Agulhas Bank and implies losses of paralarvae similar to those observed by Roberts and Mullon (2010). However, including experimental specific gravity data in repeated simulations reduced the plume length (i.e. the transport distance). This halted the particle loss to the open ocean and abbreviated dispersal from the inshore release sites.

The vertical distribution profiles from the simulations indicated that plume length, i.e. transport distance, was significantly influenced by the presence of particles in the surface layer, which actually only involved neutral particles. Reduced plume length was caused by the absence of particles in the surface layer as a result of the introduction of a greater specific gravity to the particle; deeper particles were subjected to slower currents relative to those in the surface. A consequence of this is that subsurface particles will take longer to reach the cold ridge and some feeding will be required on route, given the 4–6 d starvation threshold already determined by Vidal *et al.* (2005) and Martins *et al.* (2010).

Acknowledgements

References

Ådlandsvik, B., Coombs, S., Sundby, S., and Temple, G. 2001. Buoyancy and vertical distribution of eggs and larvae of blue whiting (*Micromesistius poutassou*): observations and modelling. Fisheries Research, 50: 59–72.

Arnold, J. M. 1965. Normal embryonic stages of the squid *Loligo pealii* (Lesueur). Biological Bulletin, 128: 24–32.

Augustyn, C. J., Lipiński, M. R., Sauer, W. H. H., Roberts, M. J., and Mitchell-Innes, B. A. 1994. Chokka squid on the Agulhas Bank: life history and ecology. South African Journal of Science, 90: 143–154.

Bell, K. N. I., and Brown, J. A. 1995. Active salinity choice and enhanced swimming endurance in 0 to 8-d-old larvae of diadromous gobies, including *Sicydium punctatum* (Pisces), in Dominica, West Indies. Marine Biology, 121: 409–417.

Blaxter, J. H. S., Danielssen, D., Moknes, E., and Øiestad, V. 1983. Description of the early development of the halibut *Hippoglossus hippoglossus* and attempts to rear the larvae past first feeding. Marine Biology, 73: 99–107.

Boebel, O., Rossby, T., Lutjeharms, J. R. E., Zenk, W., and Barron, C. 2003. Path and variability of the Agulhas Return Current. Deep Sea Research II, 50: 35–56.

Boletzky, Sv. 2003. Biology of early life stages in cephalopod molluscs. Advances in Marine Biology, 44: 144–184.

Bradbury, I. R., and Snelgrove, P. V. R. 2001. Contrasting larval transport in demersal fish and benthic invertebrates: the roles of behaviour and advective processes in determining spatial pattern. Canadian Journal of Fisheries and Aquatic Sciences, 58: 811–823.

Bryden, H. L., Beal, L. M., and Duncan, L. M. 2005. Structure and transport of the Agulhas Current and its temporal variability. Journal of Oceanography, 61: 479–492.

Cambalik, J. J., Checkley, D. M., and Kamykowski, D. 1998. A new method to measure the terminal velocity of small particles: a demonstration using ascending eggs of the Atlantic menhaden (*Brevoortia tyrannus*). Limnology and Oceanography, 43: 1722–1727.

Campbell, R. W., and Dower, J. F. 2003. Role of lipids in the maintenance of neutral buoyancy by zooplankton. Marine Ecology Progress Series, 263: 93–99.

Chang, N. 2008. Numerical ocean model study of the Agulhas Bank and the cool ridge. PhD thesis, Department of Oceanography, University of Cape Town.

Chia, F-S., Buckland-Nicks, J., and Young, C. M. 1984. Locomotion of marine larvae: a review. Canadian Journal of Zoology, 62: 1205–1222.

Conkright, M. E., Locarnini, R. A., Garcia, H. E., O'Brien, T. D., Boyer, T. P., Stephens, C., and Antonov, J. I. 2002. World Ocean Atlas 2001: objective analyses, data statistics, and figures, CD-ROM documentation. Technical Report, National Oceanographic Data Center, Silver Spring, MD.

Da Silva, A. M., Young, C. C., and Levitus, S. 1994. Atlas of surface marine data 1994, Vol. 1. Algorithms and procedures. Technical Report, US Department of Commerce, NOAA, Washington, DC.

Ellertsen, B., Solemda, P., Strømme, T., Tilseth, S., Westgård, T., Moksness, E., and Øiestad, V. 1980. Some biological aspects of cod larvae (*Gadus morhua* L.). Fiskeridirektoratets Skrifter Serie Havundersøkelser, 17: 29–47.

Franks, P. J. S. 1992. Sink or swim: accumulation of biomass at fronts. Marine Ecology Progress Series, 82: 1–12.

Q3

Gallager, S. M. 1985. Buoyancy regulation and swimming energetics in larvae of *Bankia gouldi* (Bartsch) (Teredinidae: Bivalvia). Abstracts of 77th Annual Meeting of the National Shellfish Association, p. 8.

Gallager, S. M., Manuel, J. L., Manning, D. A., and O'Dor, R. K. 1996. Ontogenetic changes in the vertical distribution of giant scallop larvae, *Placopecten magellanicus*, in 9-m deep mesocosms as a function of light, food, and temperature stratification. Marine Biology, 124: 679–692.

Hare, J. A., Walsh, H. J., and Wuenschel, M. J. 2006. Sinking rates of late-stage fish larvae: implications for larval ingress into estuarine nursery areas. Journal of Experimental Marine Biology and Ecology, 330: 493–504.

Heming, T. A., and Buddington, R. K. 1988. Yolk absorption in embryonic and larval fishes. *In* Fish Physiology, 9A, pp. 407–446. Ed. by W. S. Hoar, and D. J. Randall. Academic Press, New York. 436 pp.

Henri, M., Dodson, J. J., and Powles, H. 1985. Spatial configurations of young herring (*Clupea harengus harengus*) larvae in the St Lawrence Estuary: importance of biological and physical factors. Canadian Journal of Fisheries and Aquatic Sciences, 42: 91–104.

Hutchings, L., Beckley, L. E., Griffiths, M. H., Roberts, M. J., Sundby, S., and van der Lingen, C. 2002. Spawning on the edge: spawning grounds and nursery areas around the southern African coastline. Marine and Freshwater Research, 53: 307–318.

Kamler, E. 2008. Resource allocation in yolk-feeding fish. Reviews in Fish Biology and Fisheries, 18: 143–200.

Kelman, D., and Emlet, R. B. 1999. Swimming and buoyancy in ontogenetic stages of the cushion star *Pteraster tesselatus* (Echinodermata: Asteroidea) and their implications for distribution and movement. Biological Bulletin, 197: 309–314.

Koordinaten.de. 2008. Formula for the distance between two coordinates on Earth. http://www.koordinaten.de/english/informations/formula.shtml (last accessed 3 January 2008).

Lebreton, J. D., Burnham, K. P., Clobert, J., and Andersson, D. R. 1992. Modelling survival and testing biological hypotheses using marked animals: a unified approach with case studies. Ecological Monographs, 62: 67–118.

Lee, P. G. 1994. Nutrition of cephalopods: fueling the system. Marine and Freshwater Behaviour and Physiology, 25: 35–51.

Lee, R. F. 1991. Lipoproteins from the hemolymph and ovaries of marine invertebrates. *In* Advances in Comparative and Environmental Physiology, 7, pp. 187–208. Ed. by R. Gilles. Springer, London. 213 pp.

Lett, C., Veitch, J., van den Lingen, C., and Hutchings, L. 2007. Assessment of an environmental barrier to transport of ichthyoplankton from the southern to the northern Benguela ecosystems. Marine Ecology Progress Series, 347: 247–259.

Lett, C., Verley, P., Mullon, C., Parada, C., Brochier, T., Penven, P., and Blanke, B. 2008. A Lagrangian tool for modelling ichthyoplankton dynamics. Environmental Modelling and Software, 23: 1210–1214.

Lutjeharms, J. R. E., and Ansorge, I. 2001. The Agulhas Return Current. Journal of Marine Systems, 30: 115–138.

Magnor-Jensen, A., and Huse, I. 1991. On the changes in buoyancy of halibut *Hippoglossus hippoglossus* (L.) larvae caused by hatching—a theoretical view. Journal of Fish Biology, 39: 133–135.

Mann, K. H., and Lazier, J. R. N. 1991. Dynamics of Marine Ecosystems. Biological–Physical Interactions in the Oceans. Blackwell Scientific, Boston. 394 pp.

Martínez, G., López, V., Mettifogo, L., and Cancino, J. M. 2008. Energy source utilization by embryos and larvae of the muricid snail *Chorus giganteus* (Lesson, 1829). Journal of Experimental Marine Biology and Ecology, 354: 65–80.

Martins, R. S., Roberts, M. J., Vidal, E. A. G., and Moloney, C. L. 2010. Effects of temperature on yolk utilization by chokka squid (*Loligo reynaudii* d'Orbigny, 1839) paralarvae. Journal of Experimental Marine Biology and Ecology, 386: 19–26.

McNown, J. S., and Malaika, J. 1950. Effects of particle shape on settling velocity at low Reynolds numbers. Transactions of the American Geophysical Union, 31: 74–82.

Moore, J. K., and Villareal, T. A. 1996. Size-ascent rate relationships in positively buoyant marine diatoms. Limnology and Oceanography, 41: 1514–1520.

Nelson, D. L., and Cox, M. M. 2004. Lehninger Principles of Biochemistry, 4th edn. WH Freeman and Co., New York. 1100 pp.

Nozais, Ch., and Duchêne, J. C. 1996. Larval buoyancy and release from terebellid polychaete egg masses. Journal of Experimental Marine Biology and Ecology, 203: 209–222.

O'Dor, R. K., Foy, E. A., and Balch, N. 1986. The locomotion and energetics of hatchling squid, *Illex illecebrosus*. American Malacological Bulletin, 4: 55–60.

Oestmann, D. J., Scimeca, J. M., Forsythe, J., Hanlon, R. T., and Lee, P. G. 1997. Special considerations for keeping cephalopods in laboratory facilities. Contemporary Topics in Laboratory Animal Science, 36: 89–93.

Oosthuizen, A., and Roberts, M. J. 2009. Bottom temperature and *in situ* development of chokka squid eggs (*Loligo vulgaris reynaudii*) on mid-shelf spawning grounds, South Africa. ICES Journal of Marine Science, 66: 1967–1971.

Parada, C., van der Lingen, C. D., Mullon, C., and Penven, P. 2003. Modelling the effect of buoyancy on the transport of anchovy eggs from spawning to nursery grounds in the southern Benguela: an IBM approach. Fisheries Oceanography, 12: 170–184.

Pennington, J. T., and Emlet, R. B. 1986. Ontogenetic and diel vertical migration of a planktonic echinoid larva, *Dendraster excentricus* (Eschscholtz): occurrence, causes, and probable consequences. Journal of Experimental Marine Biology and Ecology, 104: 69–95.

Penven, P., Lutjeharms, J. R. E., and Florenchie, P. 2006. Madagascar: a pacemaker for the Agulhas Current system? Geophysical Research Letters, 33: L17609. doi:10.1029/2006GL026854.

Penven, P., Roy, C., Brundrit, G. B., Colin de Verdière, A., Fréon, P., Johnson, A. S., Lutjeharms, J. R. E., *et al.* 2001. A regional hydrodynamic model of upwelling in the southern Benguela. South African Journal of Science, 97: 472–475.

Peterson, R. H., and Metcalfe, J. L. 1977. Changes in specific gravity of Atlantic salmon (*Salmo salar*) alevins. Journal of the Fisheries Research Board of Canada, 34: 2388–2395.

Rio, M-H., and Hernandez, F. 2004. A mean dynamic topography computed over the world ocean from altimetry, in situ measurements, and a geoid model. Journal of Geophysical Research, 109: C12032. doi:10.1029/2003JC002226

Roberts, M. J. 2005. Chokka squid (*Loligo vulgaris reynaudii*) abundance linked to changes in South Africa's Agulhas Bank ecosystem during spawning and the early life cycle. ICES Journal of Marine Science, 62: 33–55.

Roberts, M. J., Barange, M., Lipiński, M. R., and Prowse, M. R. 2002. Direct hydroacoustic observations of chokka squid *Loligo vulgaris reynaudii* spawning activity in deep water. South African Journal of Marine Science, 24: 387–393.

Roberts, M. J., and Mullon, C. 2010. First ROMS–IBM simulations indicate poor recruitment in the South African squid fishery (*Loligo vulgaris reynaudii*) is caused by off-shelf losses of paralarvae. African Journal of Marine Science, 32: 71–84.

Roberts, M. J., and Sauer, W. H. H. 1994. Environment: the key to understanding the South African chokka squid (*Loligo vulgaris reynaudii*) life cycle and fishery? Antarctic Science, 6: 249–258.

Sclafani, M., Stirling, G., and Leggett, W. C. 1997. Osmoregulation, nutritional effects and buoyancy of marine fish larvae: a bioassay for assessing density changes during the earliest life history stages. Marine Biology, 129: 1–9.

Sclafani, M., Taggart, C. T., and Thompson, K. R. 1993. Condition, buoyancy and distribution of larval fish: implications for vertical migration and retention. Journal of Plankton Research, 15: 413–435.

Shchepetkin, A. F., and McWilliams, J. C. 2005. The regional oceanic modeling system (ROMS): a split-explicit, free-surface, topography-following-coordinate oceanic model. Ocean Modelling, 9: 347–404.

Song, Y. T., and Haidvogel, D. 1994. A semi-implicit ocean circulation model using a generalized topography following coordinate system. Journal of Computational Physics, 115: 228–248.

Sundby, S. 1983. A one-dimensional model for the distribution of pelagic fish eggs in the mixed layer. Deep Sea Research, 30: 645–661.

Sundby, S. 1991. Turbulence and ichthyoplankton: influence on vertical distributions and encounter rates. Scientia Marina, 61: 159–176.

Takashi, T., Kohno, H., Sakamoto, W., Miyashita, S., Murata, O., and Sawada, Y. 2006. Diel and ontogenetic body density change in Pacific bluefin tuna, *Thunnus orientalis* (Temminck and Schlegel), larvae. Aquacultural Research, 37: 1172–1179.

Tanaka, Y. 1992. Japanese anchovy eggs accumulation at the sea surface or pycnocline—observations and model. Journal of Oceanography, 48: 461–472.

Thompson, J. T., and Kier, W. M. 2001. Ontogeny of squid mantle function: changes in the mechanics of escape-jet locomotion in the oval squid, *Sepioteuthis lessoniana* Lesson, 1830. Biological Bulletin, 203: 14–26.

Trotter, A. J., Battaglene, S. C., and Pankhurst, P. M. 2005. Buoyancy control and diel changes in swim-bladder volume in cultured striped trumpeter (*Latris lineata*) larvae. Marine and Freshwater Research, 56: 361–370.

Tsukamoto, K., Yamada, Y., Okamura, A., Kaneko, T., Tanaka, H., Miller, M. J., Horie, N., *et al.* 2009. Positive buoyancy in eel leptocephali: an adaptation for life in the ocean surface layer. Marine Biology, 156: 835–846.

Vidal, E. A. G., DiMarco, F. P., and Lee, P. G. 2006. Effects of starvation and recovery on the survival, growth and RNA/DNA ratio in loliginid squid paralarvae. Aquaculture, 260: 94–105.

Vidal, E. A. G., DiMarco, F. P., Wormuth, J. H., and Lee, P. G. 2002. Influence of temperature and food availability on survival, growth and yolk utilization in hatchling squid. Bulletin of Marine Science, 71: 915–931.

Vidal, E. A. G., Roberts, M. J., and Martins, R. S. 2005. Yolk utilization, metabolism and growth in reared *Loligo vulgaris reynaudii* paralarvae. Aquatic Living Resources, 18: 385–394.

Yin, M. C., and Craik, J. C. A. 1992. Biochemical changes during development of eggs and yolk-sac larvae of herring and plaice. Chinese Journal of Oceanology and Limnology, 10: 347–358.

Young, C. M. 1995. Behaviour and locomotion during the dispersal phase of larval life. *In* Ecology of Marine Invertebrate Larvae, pp. 249–277. Ed. by L. McEdward. CRP Press, Boca Ratón, FL. 480 pp.

Zar, J. H. 1996. Biostatistical Analysis, 3rd edn. Prentice-Hall, Englewood Cliffs, NJ. 718 pp.

Zeidberg, L. D., and Hamner, W. M. 2002. Distribution of squid paralarvae, *Loligo opalescens* (Cephalopoda: Myopsida), in the southern California Bight in the three years following the 1997–1998 *El Niño*. Marine Biology, 141: 111–122.

Zeldis, J. R., Grimes, P. J., and Ingerson, J. K. V. 1995. Ascent rates, vertical distribution and a thermal history model of orange roughy, *Hoplostethus atlanticus*, eggs in the water column. Fishery Bulletin US, 93: 373–385.

Zuev, G. V. 1964. On the ability of cephalopod larvae to active movement. Zoologicheskii Zhurnal, 43: 1440–1445.